Monatshefte für Chemie 136, 77–89 (2005)
DOI 10.1007/s00706-004-0253-z

Monatshefte für Chemie
Chemical Monthly
Printed in Austria

Synthesis of Zeolite L. Tuning Size and Morphology

Arantzazu Zabala Ruiz, Dominik Brühwiler, Takayuki Ban, and **Gion Calzaferri***

Department of Chemistry and Biochemistry, University of Bern,
CH-3000 Bern 9, Switzerland

Received August 5, 2004; accepted August 12, 2004
Published online December 6, 2004 © Springer-Verlag 2004

Summary. A convenient synthesis of zeolite L is presented. The size of the crystals can be tuned between 30 and 6000 nm, spanning a volume range of seven orders of magnitude. The zeolite L crystals, which typically feature a cylindrical morphology, are synthesized with various aspect ratios ranging from elongated to disc-shaped. The importance of obtaining zeolite crystals with well-defined size and morphology is discussed in view of potential applications of zeolite L containing organic dye molecules as guests.

Keywords. Hydrothermal synthesis; Inclusion compounds; Nanostructures; Zeolites; Electron microscopy.

Introduction

Zeolites are crystalline aluminosilicates featuring defined channels and cavities. The ability to accommodate various organic and inorganic species while being transparent in the UV-Vis-NIR makes zeolites ideal host materials for supramolecular organization [1, 2]. In many cases the confinement of molecules in zeolites and the catalytic activity of surface adsorption sites lead to interesting photochemical phenomena not observed in solution [3].

Zeolite L possesses one-dimensional channels arranged in a hexagonal pattern (see Fig. 1) [4]. High-resolution electron microscopy has been used by *Ohsuna et al.* [5] to image the surface structures of zeolite L and to advance the understanding of growth processes and defects. Materials obtained by the inclusion of organic dye molecules into the channels of zeolite L feature a variety of intriguing properties, ranging from increased dye stability to photonic antenna functions and optical anisotropy [6]. The potential of dye-zeolite L composites is fully

* Corresponding author. E-mail: gion.calzaferri@iac.unibe.ch

source: https://doi.org/10.7892/boris.30790 | downloaded: 12.10.2024

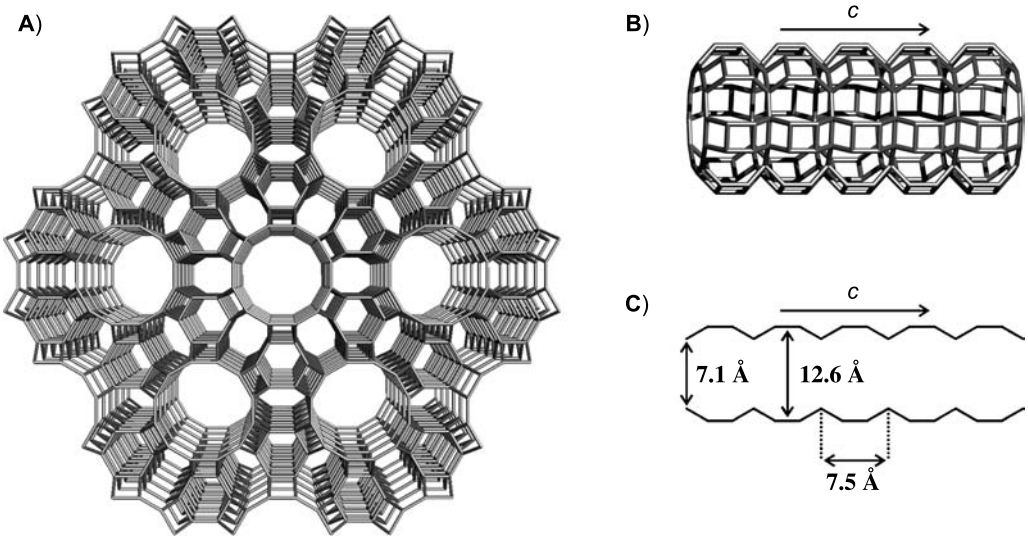

Fig. 1. A) Zeolite L framework projected along the *c*-axis; B) side view of the main channel; C) its dimensions

exploited by tuning the size and morphology of the zeolite crystals according to the requirements of a given application. Small dye-loaded zeolite crystals (<300 nm) are potential functional pigments, whereas large crystals (>1 μm) are used for the investigation of dye arrangements by optical microscopy [7, 8]. Disc-shaped crystals, *i.e.*, crystals of low aspect ratio (=length/diameter), lead to oriented monolayers upon deposition onto a substrate, whereas crystals of high aspect ratio allow for alignment on microstructured surfaces, thereby opening possibilities for producing macroscopic areas of oriented guest molecules. The successful assembly of aligned zeolite monolayers largely depends on the ability to obtain zeolite crystals with narrow size distribution and well-defined morphology [9].

Results and Discussion

Despite the very useful collection of verified syntheses of zeolitic materials [10], recipes for zeolite synthesis are often difficult to follow for the non-specialist and frequently involve elaborate equipment. We will in the following present a convenient and reproducible procedure for the synthesis of zeolite L. Starting from a standard routine (see Fig. 2), the size and morphology of the products are tuned by changing the gel composition (H_2O/SiO_2 and K_2O/SiO_2 ratios) as well as other synthesis parameters such as the type of silica source and crystallization with or without agitation (dynamic or static). Table 1 gives an overview of the obtained products. Details concerning the separate steps of the syntheses are outlined in the Experimental. We have divided the products according to their particle size into three groups which are discussed in the following subsections.

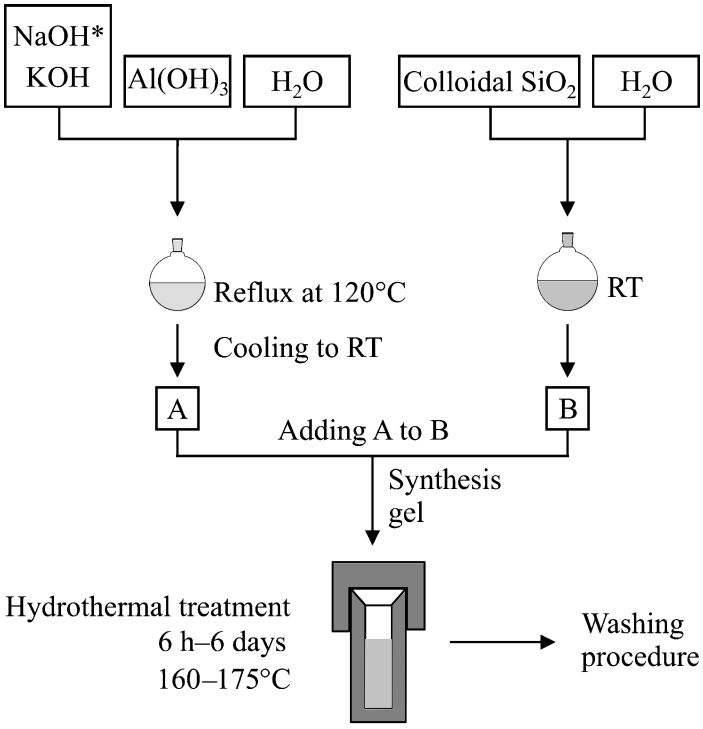

Fig. 2. General scheme of the zeolite L synthesis procedure; details are given in the Experimental

Table 1. Synthesis and product characteristics

Crystal length along *c*-axis/nm	Starting gel composition K_2O:Al_2O_3:SiO_2:H_2O	Crystallization			Silica source[b]	Variation	Aspect ratio[c]
		t/h	T/°C	cond.[a]			
30–70	9.34:1.00:20.20:412.84	6	170	d	AO	–	1.0
200–550	3.17:1.00:9.83:168.52	42	160	d	AO	Mg^{2+}	0.6
400–1300	*2.55*:1.00:9.83:165.60	42	160	d	AO	Increase of	1.3
	2.70:1.00:9.83:165.60	42	160	d	AO	alkalinity	1.2
	2.83:1.00:9.83:165.60	42	160	d	AO		0.8
	3.13:1.00:9.83:165.60	42	160	d	AO		0.6
250–450	5.40:*5.50*:1.00:30.00:416.08[d]	48	160	d	L	NaOH	0.3
1000–3000	2.99:1.00:10.70:*182.00*	144	160	s	AK	Increase of	1.1
	2.99:1.00:10.70:*194.60*	144	160	s	AK	H_2O content	1.1
	2.99:1.00:10.70:*199.20*	144	160	s	AK		1.2
	2.99:1.00:10.70:*250.70*	144	160	s	AK		1.8
	2.99:1.00:10.70:*299.70*	144	160	s	AK		1.7
	2.99:1.00:10.70:*332.40*	144	160	s	AK		1.2
	2.55:1.00:9.72:161.30	144	160	s	AK	–	2.0
4000–6000	2.21:1.00:9.00:164.60	72	175	s	L	Al source	2.6

[a] Crystallization conditions: d = dynamic, s = static; [b] AO = Aerosil OX-50, AK = Aerosil K-330, L = Ludox HS-40; [c] calculated from the mean length and the mean diameter; [d] 5.40 K_2O–5.50 Na_2O–1.00 Al_2O_3–30.00 SiO_2–427.00 H_2O

Small Crystals

To obtain zeolite L nanocrystals we performed the synthesis as reported in Ref. [11], except for changes in the starting gel composition and the silica source (Aerosil OX-50). Dynamic crystallization conditions were applied for 6 h at 170°C. A highly alkaline molar composition 9.34 K_2O–1.00 Al_2O_3–20.20 SiO_2–412.84 H_2O was used, yielding zeolite crystals with a size of about 30 nm which tend to agglomerate into larger clusters of 80 to 100 nm [12]. Figure 3 shows the scanning electron microscopy image (SEM) and the transmission electron microscopy image (TEM) of these crystals, the latter even resolving the channel structure. The X-ray diffraction (XRD) pattern showed the line broadening expected for such a small particle size.

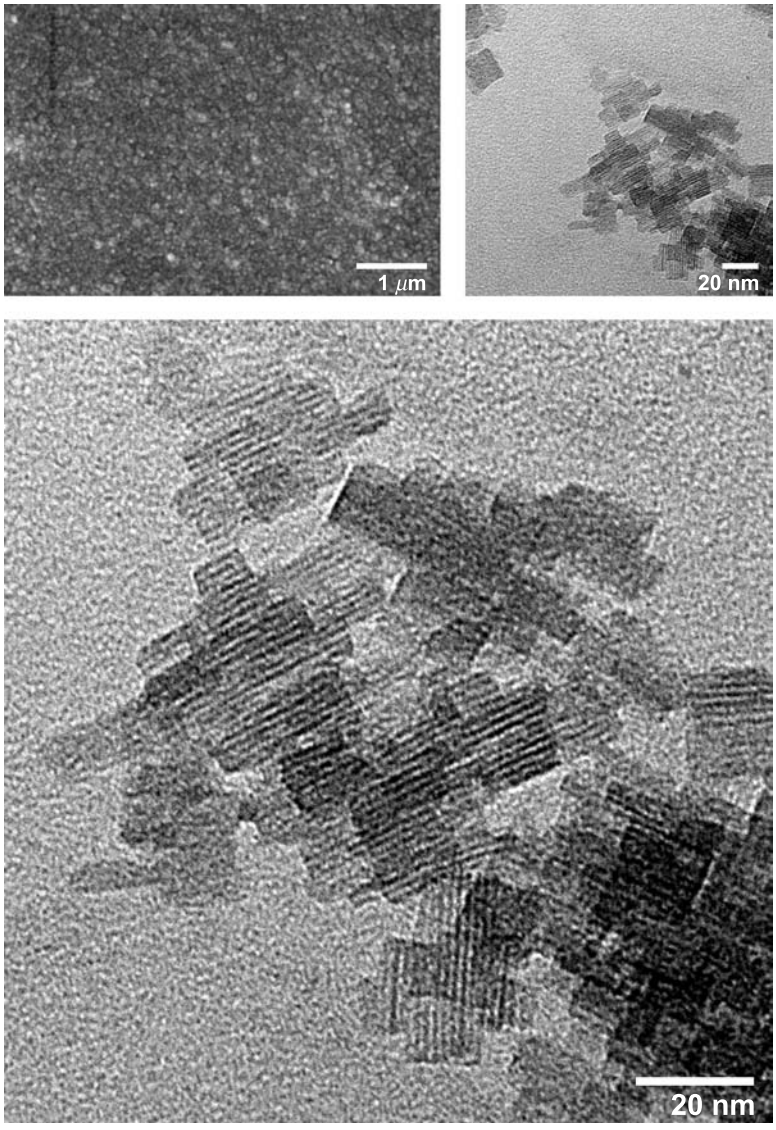

Fig. 3. TEM images of zeolite L nanocrystals; top left: SEM image

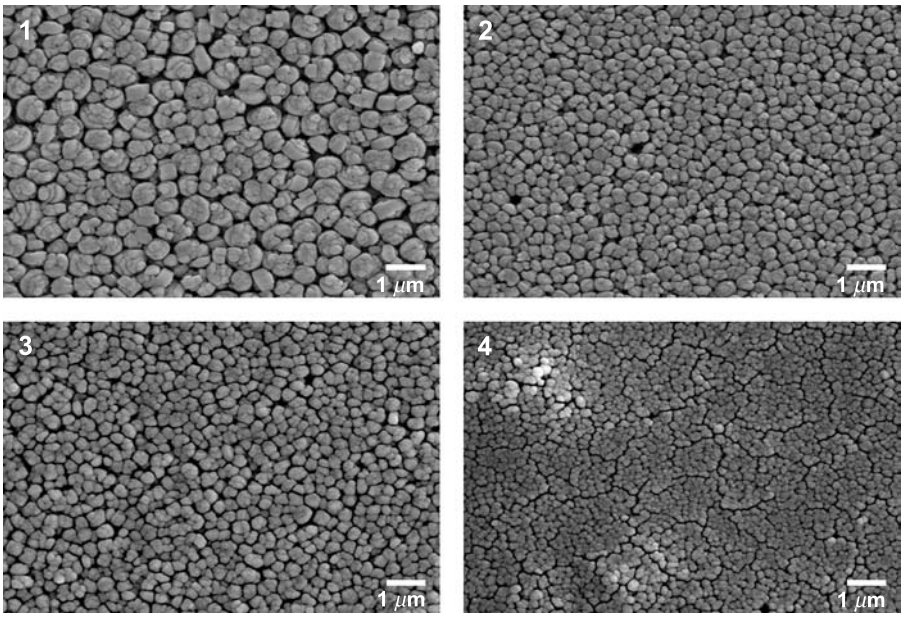

Fig. 4. SEM images of zeolite L crystals synthesized with the same gel composition and seeded with different amounts of Mg^{2+}: 1) 0 ppm, 2) 5 ppm, 3) 10 ppm, 4) 20 ppm

Medium Size Crystals

Crystals 200–550 nm: 'cauliflower like' morphology. A synthesis mixture was prepared as described in Ref. [13] with a molar composition of 3.17 K_2O–1.00 Al_2O_3–9.83 SiO_2–168.52 H_2O. The silica suspension (Aerosil OX-50) was seeded with Mg^{2+} ($Mg(NO_3)_2 \cdot 6H_2O$) and the synthesis mixture was crystallized at 160°C for 42 h under dynamic conditions. The same product was obtained upon reducing the crystallization time and increasing the rotation speed by a factor of two. Figure 4 shows the influence of the addition of small amounts of Mg^{2+} to the reaction mixture. The introduction of Mg^{2+} into the zeolite synthesis mixture reduces the occurrence of impurity phases and stimulates the formation of small crystals. Unfortunately, part of the cylinder morphology is lost at the same time. Agglomeration of zeolite crystals occurs at Mg^{2+} concentrations above 10 ppm.

Crystals 400–1300 nm. It has been reported that the particle size of zeolite L decreases with increasing alkalinity, *i.e.*, increasing K_2O/Al_2O_3 ratio [14]. We studied this effect by starting with the formal composition of 2.55 K_2O–1.00 Al_2O_3–9.83 SiO_2–165.60 H_2O and increasing the K_2O content in four steps up to 3.13 (using Aerosil OX-50 as silica source). The synthesis mixtures were crystallized at 160°C for 42 h under dynamic conditions. Figure 5 shows that increasing the alkalinity results not only in crystals of lower aspect ratio, but also in an increasing intergrowth at the crystal ends. Despite the fact that this intergrowth reduces the morphological quality of the crystals, the overall cylindrical shape is well preserved.

Dynamic and static crystallization conditions appeared to influence the morphology of crystals larger than 1000 nm, whereas there was no significant influence on crystals below this size. Figure 6 shows SEM images of two samples prepared

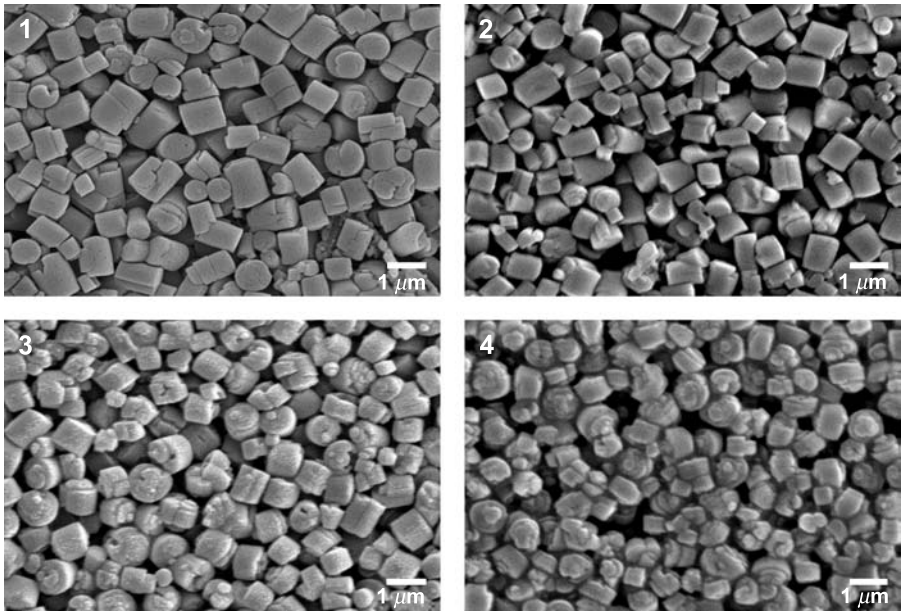

Fig. 5. SEM images of zeolite L crystals synthesized with the gel composition a K_2O–1.00 Al_2O_3–9.83 SiO_2–165.60 H_2O; 1) $a = 2.55$, 2) $a = 2.70$, 3) $a = 2.83$, 4) $a = 3.13$

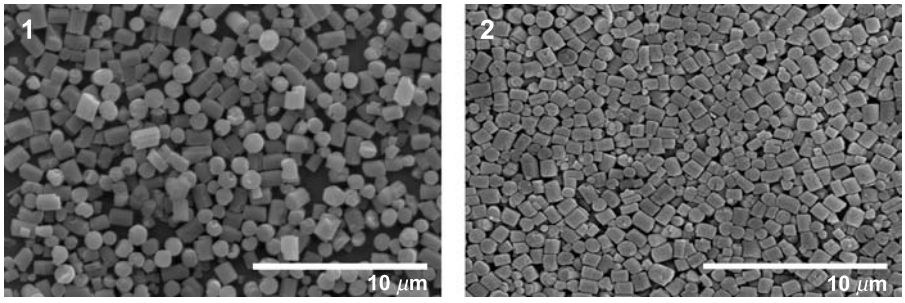

Fig. 6. SEM images of zeolite L crystals synthesized with the gel composition 2.55 K_2O–1.00 Al_2O_3–9.83 SiO_2–165.60 H_2O and crystallized 1) under static conditions, 2) under dynamic conditions

with the same starting gel composition, but with different crystallization conditions. Obviously, dynamic crystallization conditions yield a product of lower quality.

Crystals 250–450 nm: disc-shaped morphology. A synthesis mixture with the composition 5.40 K_2O–5.50 Na_2O–1.00 Al_2O_3–30.00 SiO_2–416.08 H_2O [15] was prepared. Dynamic crystallization conditions were applied at 160°C for 48 h. The best results, *i.e.*, a homogeneous distribution of disc-shaped zeolite L crystals, were obtained with Ludox as the silica source (see Fig. 7).

Large Crystals

Crystals 1–3 μm. Crystals with cylindrical morphology were obtained by starting with a gel composition of 2.99 K_2O–1.00 Al_2O_3–10.70 SiO_2–182.00 H_2O and increasing

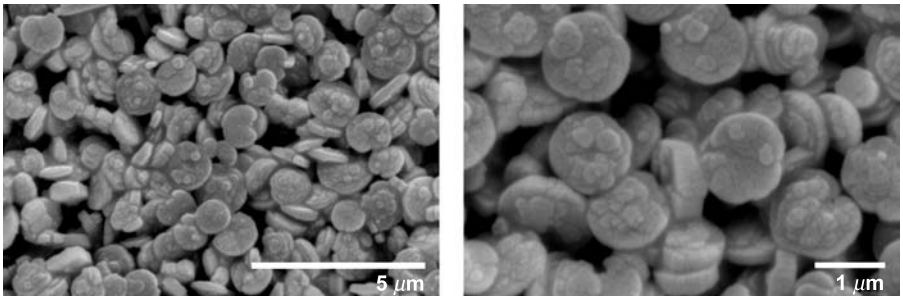

Fig. 7. SEM images of disc-shaped zeolite L crystals

the amount of water in six steps up to 332.40 (using Aerosil K-330 as silica source). The synthesis mixtures were crystallized at 160°C for 6 days under static conditions. By increasing the water content of the starting gel we were able to increase the size of the crystals without reducing the morphological quality (see Fig. 8).

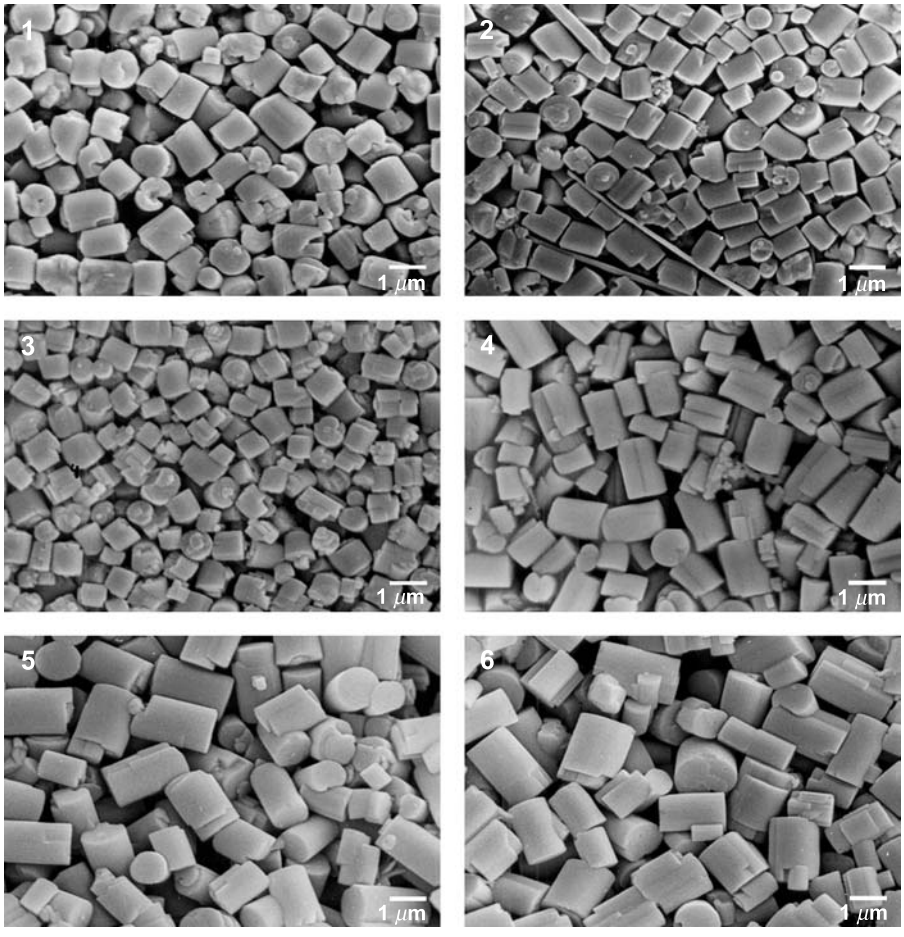

Fig. 8. SEM images of zeolite L crystals synthesized with the gel composition 2.99 K_2O–1.00 Al_2O_3–10.70 SiO_2–d H_2O; 1) $d = 182.00$, 2) $d = 194.60$, 3) $d = 199.20$, 4) $d = 250.70$, 5) $d = 299.70$, 6) $d = 332.40$

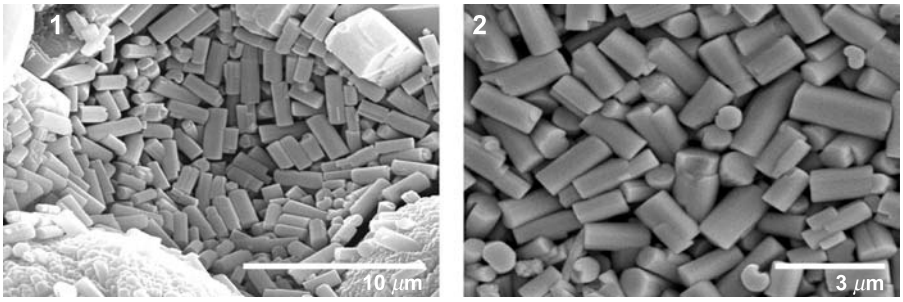

Fig. 9. SEM images of zeolite L crystals synthesized with the gel composition 2.55 K_2O–1.00 Al_2O_3–9.72 SiO_2–161.30 H_2O; 1) product obtained after crystallization and before separation; 2) after separation from the impurity phase by sedimentation

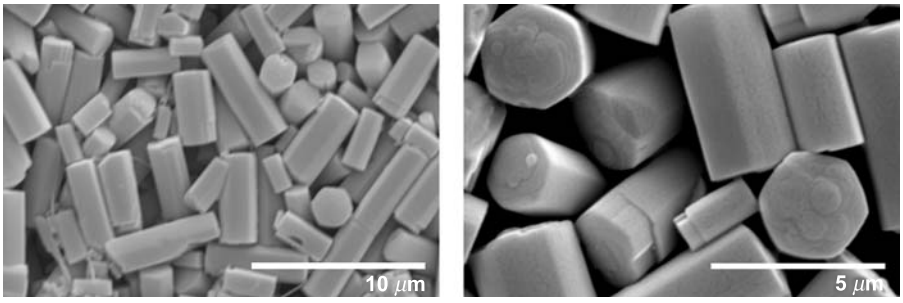

Fig. 10. SEM images of large zeolite L crystals

A composition of 2.55 K_2O–1.00 Al_2O_3–9.72 SiO_2–161.30 H_2O resulted in 3 μm cylindrical zeolite L crystals which were obtained together with an impurity phase. The zeolite L crystals were separated from the impurity phase by sedimentation (see Fig. 9).

Crystals 4–6 μm. We followed a slightly different procedure to obtain these crystals, starting with a molar composition of 2.21 K_2O–1.00 Al_2O_3–9.00 SiO_2–164.60 H_2O. A homogeneous distribution of cylindrical crystals with hexagonal cross-section and smooth surfaces were obtained (see Fig. 10). Details are given in the Experimental.

The size of zeolite L crystals can be tuned in the range of 30 to 6000 nm by variation of a convenient standard procedure. By increasing the alkalinity for a given molar composition, crystals smaller than 1 μm were obtained, although the control of the morphology was difficult in this case. Well-shaped cylindrical crystals larger than 1 μm were prepared by increasing the amount of water for a given molar composition. Static conditions during crystallization appeared to be ideal for this size regime, whereas no significant difference between static and dynamic conditions was observed for smaller crystals. Zeolite L crystals are usually obtained with aspect ratios above one. We have shown that by careful control of the starting gel composition and the crystallization conditions, as well as an appropriate choice of the silica source, disc-shaped crystals can be synthesized. A disc-shaped morphology is an important prerequisite for the preparation of oriented

monolayers of zeolite L and therefore essential for optimizing the use of dye-zeolite composites as photonic antenna systems. Transport of electronic excitation energy by the chains of dye molecules occurs preferentially along the main channels, *i.e.*, along the *c*-axis of dye-loaded zeolite L [6]. An arrangement consisting of zeolite L crystals oriented with their *c*-axes perpendicular to a substrate is thus desirable for the efficient transport of electronic excitation energy towards the zeolite-substrate interface. We have found that the morphology of the zeolite L crystals determines the degree of orientation. Whereas an average aspect ratio of 1.3 resulted in monolayers with only 45% of the crystals in the desired orientation, disc-shaped zeolites with an aspect ratio of 0.3 gave monolayers with close to perfect orientation. The combination of such oriented antennae with a semiconducting substrate is of considerable interest for the preparation of sensitized solar cells and the development of novel light emitting diodes (LEDs) [16]. Embedding of dye-loaded zeolite nanocrystals into thin film solar cells is another possibility to achieve sensitization. Concerning the potential applications of guest-zeolite composites, the control of the size and morpholgy of the zeolitic host is in any case essential for achieving an ideal interaction with external devices.

The synthesis of large zeolite L crystals with well-defined morphology has proven to be especially useful for analytical purposes by allowing for a detailed analysis of the distribution and interaction (energy transfer processes) of guest molecules by time- and space-resolved fluorescence measurements [7] and by offering possibilities for visualizing the intrachannel diffusion of dye molecules [17].

Experimental

Materials

We have tested three different silica sources: Two kinds of colloidal silica sol (Ludox HS-40 from Aldrich, 40% SiO_2 and Aerosil K-330 from Degussa, 30% SiO_2) and fine silica powder (Aerosil OX-50 from Degussa). For the latter, a colloidal suspension containing 30% SiO_2 was freshly prepared before the synthesis. Two different alumina sources were used: Aluminum hydroxide (Fluka, purum >99%) and aluminum powder (Fluka, purum >99%), the latter being only used for one specific synthesis. To introduce alkali metal cations we used KOH (Fluka, Micro Select pellets, $\geq$86%) and, depending on the requirements, NaOH (Merck, pellets GR for analysis, >99%). Throughout the synthesis doubly distilled water was used.

Calculations

In order to achieve a high reproducibility, the composition of the starting gel has to be strictly adhered to. In the zeolite literature there are, however, different procedures to calculate the required amounts of chemicals from a given gel composition. In many cases the assumptions on which these procedures are based are not clearly set forth. In the following we will therefore describe in detail our procedure to calculate the amounts of required starting material for a given molar composition a K_2O–b Al_2O_3–c SiO_2–d H_2O. It is important to note that the composition of the reaction mixture is given as a ratio of oxides. Hydroxides must therefore be considered as oxides plus water, *e.g.*, KOH results in $1/2$ K_2O and $1/2$ H_2O. The amount of water introduced into the reaction mixture by the hydroxides has to be

accounted for. The required amounts of KOH, $Al(OH)_3$, SiO_2, and H_2O are given by Eqs. (5)–(8) based on Eqs. (1)–(4).

$$\mathrm{Mol_{KOH}} = 2a \tag{1}$$

$$\mathrm{Mol_{Al(OH)_3}} = 2b \tag{2}$$

$$\mathrm{Mol_{SiO_2}} = c \tag{3}$$

$$\mathrm{Mol_{TotH_2O}} = d \tag{4}$$

$$\mathrm{Weight_{KOH}} = \frac{\mathrm{Mol_{KOH}} \cdot \mathrm{MW_{KOH}}}{\mathrm{P_{KOH}}} \tag{5}$$

$$\mathrm{Weight_{Al(OH)_3}} = \frac{\mathrm{Mol_{Al(OH)_3}} \cdot \mathrm{MW_{Al(OH)_3}}}{\mathrm{P_{Al(OH)_3}}} \tag{6}$$

$$\mathrm{Weight_{SiO_2}} = \mathrm{Mol_{SiO_2}} \cdot \mathrm{MW_{SiO_2}} \tag{7}$$

$$\mathrm{Weight_{TotH_2O}} = \mathrm{Mol_{H_2O}} \cdot \mathrm{MW_{H_2O}} \tag{8}$$

$\mathrm{MW_{KOH}}$, $\mathrm{MW_{Al(OH)_3}}$, $\mathrm{MW_{SiO_2}}$, and $\mathrm{MW_{H_2O}}$ are the molar masses. $\mathrm{P_{KOH}}$, $\mathrm{P_{Al(OH)_3}}$, and $\mathrm{P_{SiO_2}}$ are the respective purities. $\mathrm{P_{SiO_2}}$ specifically refers to the SiO_2 content of the silica suspension (see below). The total amount of water is distributed among the silica suspension and the potassium-aluminate solution as follows by Eqs. (9) and (10).

$$\mathrm{Weight_{H_2O\,SiO_2susp}} = \frac{\mathrm{Weight_{SiO_2}}(1 - \mathrm{P_{SiO_2}})}{\mathrm{P_{SiO_2}}} \tag{9}$$

$$\begin{aligned}\mathrm{Weight_{H_2OKAl}} = \mathrm{Weight_{TotH_2O}} - \Big[&\mathrm{Weight_{H_2O\,SiO_2susp}} + \mathrm{Weight_{Al(OH)_3}}(1 - \mathrm{P_{Al(OH)_3}}) \\ &+ \mathrm{Weight_{KOH}}(1 - \mathrm{P_{KOH}}) + \frac{1}{2} \cdot \mathrm{Mol_{KOH}} \cdot \mathrm{MW_{H_2O}} \\ &+ \frac{3}{2} \cdot \mathrm{Mol_{Al(OH)_3}} \cdot \mathrm{MW_{H_2O}}\Big]\end{aligned} \tag{10}$$

The total weight of the starting gel is then given by Eq. (11).

$$\mathrm{Weight_{Tot}} = \mathrm{Weight_{KOH}} + \mathrm{Weight_{Al(OH)_3}} + \mathrm{Weight_{SiO_2}} + \mathrm{Weight_{H_2O\,SiO_2susp}} + \mathrm{Weight_{H_2OKAl}} \tag{11}$$

The total weight can be scaled to the capacity of the crystallization vessels. We typically worked with 40 g of starting gel. The addition of further hydroxides to the synthesis mixture (NaOH for the preparation of disc-shaped crystals) has to be taken into account accordingly.

Synthesis

Zeolite L crystals were synthesized in a hydrothermal process, *i.e.*, crystallization took place in an aqueous system containing the necessary reactants at high temperatures. Figure 2 illustrates the standard procedure. Calculated amounts of aluminum hydroxide, potassium hydroxide, and, in specific cases sodium hydroxide, were added to a precise amount of water and refluxed for 3 h at 120°C resulting in a clear solution. A silica suspension was prepared separately with a calculated amount of colloidal silica when Ludox was used. For silica powder, we added a calculated amount of silica to water and suspended it for 15 min at 18000 $\mathrm{min^{-1}}$ (Turrax mixer, IKA). This suspension was left between 0.5 to 1 h and again mixed for 10 min before use. After letting the potassium (sodium)

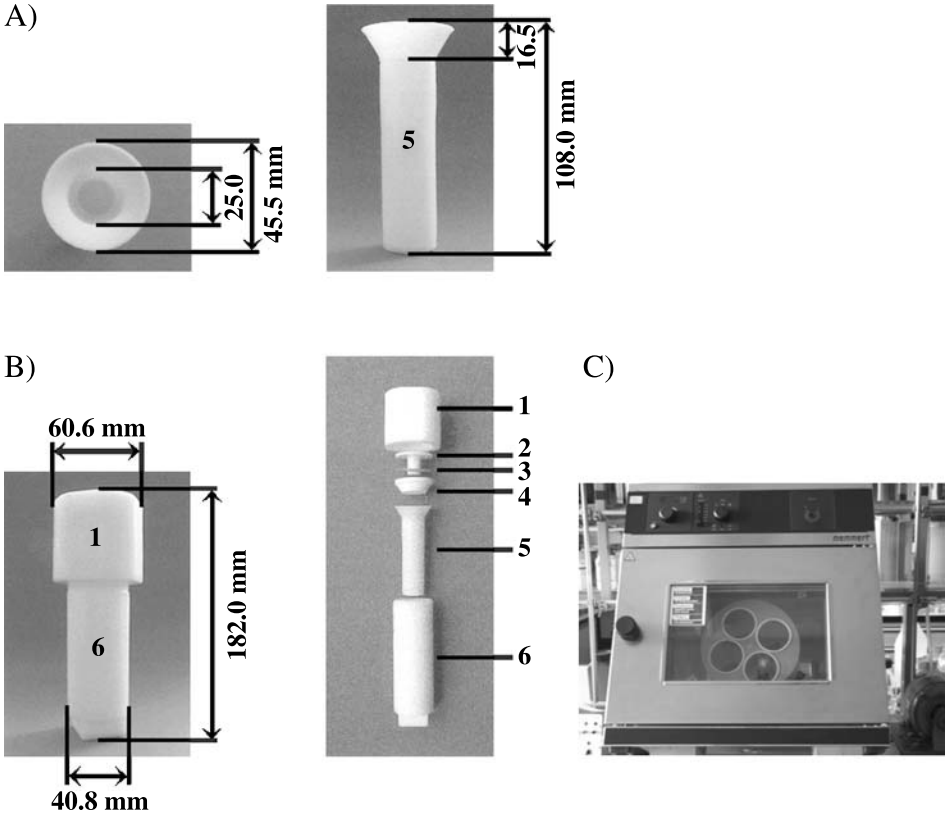

Fig. 11. Experimental setup: A) cylindrical *PTFE* vessel, left: front view, right: top view; B) *PTFE* pressure vessel, MLS GmbH, HPV80, 50 ml, 60 bar, left: assembled *PTFE* pressure vessel, right: dismantling of the *PTFE* pressure vessel: 1) screw cap, 2) pressure plate, 3) elastomer ring, 4) lid with 2, 3, and 4 mm rupture discs, 5) insert, 6) pressure vessel with a wall thickness of 10.05 mm; C) oven with rotating device

aluminate solution cool to room temperature, we added it to the colloidal silica suspension under vigorous stirring and continued stirring for 3 to 6 min. The resulting homogeneous opaque gel is the final gel before crystallization. This gel was then transferred into a cylindrical poly(tetrafluoroethylene) (*PTFE*) vessel, which was itself placed in a tight *PTFE* pressure vessel. Crystallization took place at 160°C in an oven equipped with a rotating device for allowing the application of dynamic conditions (see Fig. 11). The rotating device consists of a holder for the pressure vessels and is mounted at an angle of approximately 30°. The rotation during crystallization was found to considerably reduce the reaction time [14]. For dynamic conditions, a rotation speed of $20\,\mathrm{min}^{-1}$ was typically applied.

After crystallization the pressure vessel was cooled in ice for 1 h before opening. The product was washed several times with approximately 250 ml of boiling water and centrifuged until the *pH* of the supernatant became neutral. The crystals were dried for approximately 16 h at 80°C in air yielding between 5 and 8 g of material. Subsequent ion exchange was performed by suspending the material in 70 ml of water and adding 4.0 g of KNO_3. After stirring this suspension for 5 h at about 50°C, we washed and centrifuged it until the *pH* of the supernatant became neutral. Finally, the crystals were dried in air for 16 h at 80°C. A typical variation of this procedure is the change of the composition of the starting gel, specifically K_2O/Al_2O_3 and H_2O/Al_2O_3 ratios.

We followed a slightly different procedure to obtain 6 μm crystals (see Fig. 12). The potassium aluminate solution was prepared as follows: Potassium hydroxide was added to water and stirred at 0°C

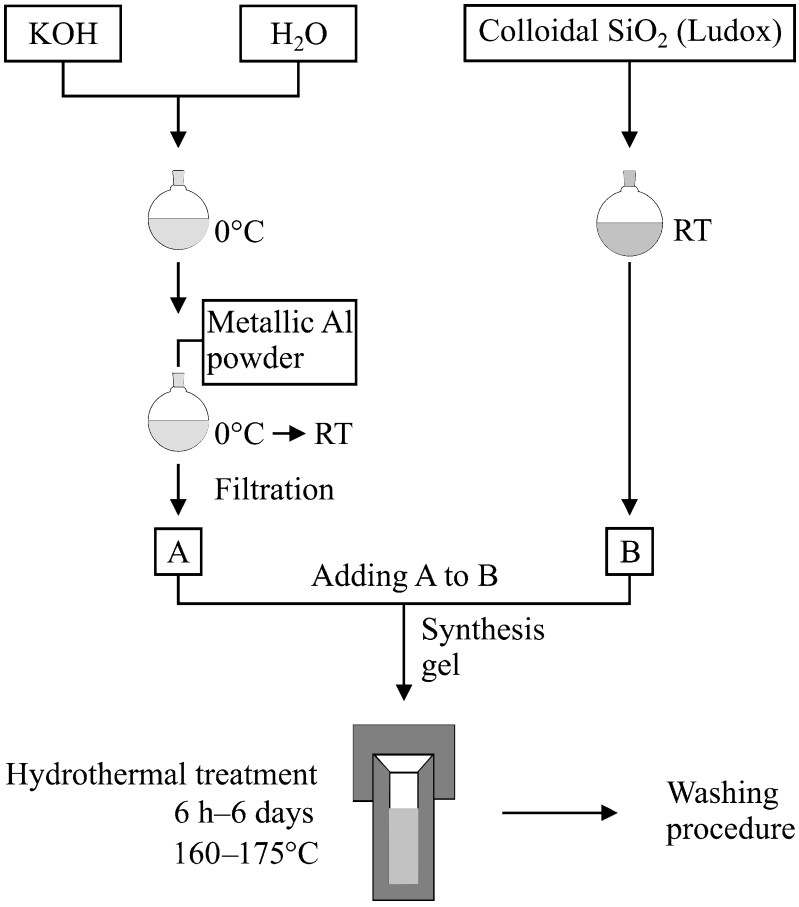

Fig. 12. Synthesis procedure for obtaining 6 μm zeolite L crystals

(on ice) for 5 min. Next, metallic aluminum powder was added under a N_2 flow and stirred at 0°C for further 15 min. After letting the solution warm to room temperature, it was stirred at this temperature for 1.5 h under N_2. The resulting solution was filtered for removing $Fe(OH)_3$, which is due to Fe as an impurity in Al, until a clear solution was obtained (between one and two times). This solution was added to the silica suspension (Ludox) under stirring. The final gel was transferred to the *PTFE* vessel for crystallization at 175°C for 72 h under static conditions. Recovering of the product was conducted as explained above.

For the synthesis of small zeolite L crystals we applied the usual procedure except for adding KOH to the silica colloidal suspension in order to increase the alkalinity of the starting gel. Potassium-silica suspension and potassium-aluminate solution were refluxed separately for 15 h before mixing. Another possibility to reduce the size of the zeolite L crystals is by adding Mg^{2+} to the silica suspension.

Characterization

The following experiment was performed to conveniently check the success of a zeolite L synthesis. When zeolite L is added to an aqueous solution of thionine, aggregates of the dye immediately form on the external zeolite surface [18]. Upon boiling the sample for about 1 min a sudden colour change from violet to blue is observed. This effect is due to the insertion of the dye molecules into the zeolite L channels where they can exist as monomers only. The blue colour remains after cooling to room temperature. If the test is negative (no colour change), the more involved characterization measurements

can be skipped. We have found that the thionine test is very reliable, except for very small crystals, where the results are not always conclusive.

The materials were analysed by X-ray powder diffraction XRD (Guinier-camera de Wolff Mk.IV, CuKα radiation, ENRAF-NONIUS) for phase identification. The obtained patterns were compared with a standard pattern of commercial zeolite L (Union Carbide or/and UOP). The morphology of the crystalline phase was examined by means of scanning electron microscopy SEM (JOEL JSM 840 and Hitachi S-3000N). Small crystals were examined by transmission electron microscopy TEM (Hitachi H-600-2 and Philips XL30 ESEM-FEG). Energy dispersive X-ray measurements EDX (NORAN TN 5402 and NORAN SIX NSS200) allowed for the determination of the elemental composition of the products.

Acknowledgements

We appreciate the assistance of Dr. *Massoud Dadras* (Institute of Microtechnology, University of Neuchâtel) for the acquisition of TEM images and his helpful advice concerning electron microscopy. We also acknowledge the kind support of *Beatrice Frey* (SEM and XRD) and *René Bühler* (expertise in zeolite synthesis). Financial support was provided by the Swiss Federal Office of Energy (project nr. 36846), the "Stiftung der Portland Cementfabrik Laufen, Switzerland", and the Swiss Federal Office for Education and Science (European Union Research Training Network *Nanochannel*).

References

[1] Brühwiler D, Calzaferri G (2004) Microporous Mesoporous Mater **72**: 1
[2] Schulz-Ekloff G, Wöhrle D, van Duffel B, Schoonheydt RA (2002) Microporous Mesoporous Mater **51**: 91
[3] Hashimoto S (2003) J Photochem Photobiol C: Photochem Rev **4**: 19
[4] a) Breck DW (1974) Zeolite Molecular Sieves. Wiley, New York; b) Baerlocher C, Meier WM, Olson DH (2001) Atlas of Zeolite Framework Types. Elsevier
[5] a) Ohsuna T, Horikawa Y, Hiraga K, Terasaki O (1998) Chem Mater **10**: 688; b) Ohsuna T, Slater B, Gao F, Yu J, Sakamoto Y, Zhu G, Terasaki O, Vaughan DEW, Qiu S, Catlow CRA (2004) Chem Eur J **10**: 5031
[6] Calzaferri G, Huber S, Maas H, Minkowski C (2003) Angew Chem Int Ed **42**: 3732
[7] Pauchard M, Huber S, Méallet-Renault R, Maas H, Pansu R, Calzaferri G (2001) Angew Chem Int Ed **40**: 2839
[8] Calzaferri G, Maas H, Pauchard M, Pfenniger M, Megelski S, Devaux A (2002) Advances in Photochemistry **27**: 1
[9] Ha K, Park JS, Oh KS, Zhou YS, Chun YS, Lee YJ, Yoon KB (2004) Microporous Mesoporous Mater **72**: 91
[10] Robson H, Lillerud KP (2001) Verified Syntheses of Zeolitic Materials. Elsevier
[11] Meng X, Zhang Y, Meng C, Pang W (1993) Proc 9th Int Zeolite Conf. Montreal, p 297
[12] a) Tsapatsis M, Okubo T, Lovallo M, Davis ME (1995) Mater Res Soc Symp Proc **371**: 21; b) Tsapatsis M, Lovallo M, Okubo T, Davis ME, Sadakata M (1995) Chem Mater **7**: 1734
[13] Verduijn JP (1996) US Patent 5 491 119
[14] Megelski S, Calzaferri G (2001) Adv Funct Mater **11**: 277
[15] Ko YS, Chang SH, Ahn WS (2001) Stud Surf Sci Catal **135**: 279
[16] Calzaferri G, Pauchard M, Maas H, Huber S, Khatyr A, Schaafsma T (2002) J Mater Chem **12**: 1
[17] Pfenniger M, Calzaferri G (2000) Chem Phys Chem **1**: 211
[18] Calzaferri G, Brühwiler D, Megelski S, Pfenniger M, Pauchard M, Hennessy B, Maas H, Devaux A, Graf U (2000) Solid State Sciences **2**: 421